









Photonic cellular automaton simulation of relativistic quantum fields: Observation of *Zitterbewegung*Alessia Suprano ^{1,*} Danilo Zia ^{1,*} Emanuele Polino ^{1,2} Davide Poderini ^{1,3} Gonzalo Carvacho ¹ Fabio Sciarrino ^{1,†}
Matteo Lugli ⁴ Alessandro Bisio ⁴ and Paolo Perinotti ^{4,‡}¹*Dipartimento di Fisica, Sapienza Università di Roma, Piazzale Aldo Moro 5, I-00185 Roma, Italy*²*Centre for Quantum Dynamics and Centre for Quantum Computation and Communication Technology, Griffith University, Brisbane, Queensland 4111, Australia*³*International Institute of Physics, Federal University of Rio Grande do Norte, P. O. Box 1613, 59078-970 Natal, Rio Grande do Norte, Brazil*⁴*QUIT Group, Dipartimento di Fisica, Università degli Studi di Pavia, and INFN Sezione di Pavia, Via Bassi 6, 27100 Pavia, Italy*

(Received 25 October 2022; accepted 12 April 2024; published 5 August 2024)

Quantum cellular automaton (QCA) is a model for universal quantum computation and a natural candidate for digital quantum simulation of relativistic quantum fields. Here we introduce the first photonic platform for implementing QCA simulation of a free relativistic Dirac quantum field in $1 + 1$ dimension, through a Dirac quantum cellular automaton (DQCA). Encoding the field position degree of freedom in the orbital angular momentum (OAM) of single photons, our state-of-the-art setup experimentally realizes eight steps of a DQCA, with the possibility of having complete control over the input OAM state preparation and the output measurement making use of two spatial light modulators. Therefore, studying the distribution in the OAM space at each step, we were able to reproduce the time evolution of the free Dirac field observing the *Zitterbewegung*, an oscillatory movement extremely difficult to see in a real-case experimental scenario that is a signature of the interference of particle and antiparticle states. The accordance between the expected and measured *Zitterbewegung* oscillations certifies the simulator performances, paving the way towards the application of photonic platforms to the simulation of more complex relativistic effects.

DOI: [10.1103/PhysRevResearch.6.033136](https://doi.org/10.1103/PhysRevResearch.6.033136)**I. INTRODUCTION**

The notion of a cellular automaton was introduced by von Neumann [1], with the purpose of showing how a simple local update rule for an array of cells containing bits (or larger information carriers) can produce complex behaviors on a macroscopic scale. The quantum version of cellular automata, the quantum cellular automaton (QCA) [2–6], was first envisaged by Feynman in his famous paper [7], where he immediately proposes their use as quantum simulators. A QCA consists of a lattice of finite-dimensional quantum systems, along with an evolution occurring in discrete steps, which can be summarized in a local update rule, i.e., involving only a finite neighborhood in the update of a given cell (see Fig. 1).

Recently, quantum cellular automata have attracted great interest due to their potential in quantum computation [8–10] and because they are universal digital quantum simulators [11–20]—by this terminology we mean that a finite portion

of space-time is simulated via a discrete network of finite-dimensional systems, of size proportional to the volume of the region of interest, following e.g., Refs. [7,21]. In this context, special attention was paid to the single-particle sector of QCAs whose dynamics reduces to a discrete-time quantum walk (DTQW) [22]. DTQWs are useful for quantum computation [23–26] and simulation [27–32], which makes them worth realizing in their own right. As the single-particle sector of a QCA, DTQWs can simulate free quantum relativistic field theories and relevant effects thereof [33–38].

Several platforms, ranging from cold atoms [39] to trapped ions [40,41] to photonics systems [28,31,42–53], have been employed to implement DTQWs. In this paper, we focus on the experimental realization of the Dirac quantum Cellular automaton (DQCA) [36,54,55], which is a fermionic cellular automaton which recovers the dynamics of a free Dirac field in the small wave-vector regime. The digital simulation of the special instance of its evolution on localized input states was pioneered in Ref. [56] on a trapped-ion quantum computer.

In this work, we implement the single-particle sector of a QCA with the same dispersion relation as that of the DQCA, corresponding to a DTQW, using a photonic platform based on the scheme proposed in Ref. [35]. We use the orbital angular momentum (OAM) of light to encode the *walker* system that is directly linked to the position of the Dirac particle, while the *coin* is codified in the polarization degree of freedom. The structured wave front characterizing OAM states and their high-dimensionality motivate the wide applications that these states have found both in the classical

*These authors equally contributed to this work.

†Contact author: fabio.sciarrino@uniroma1.it‡Contact author: paolo.perinotti@unipv.it

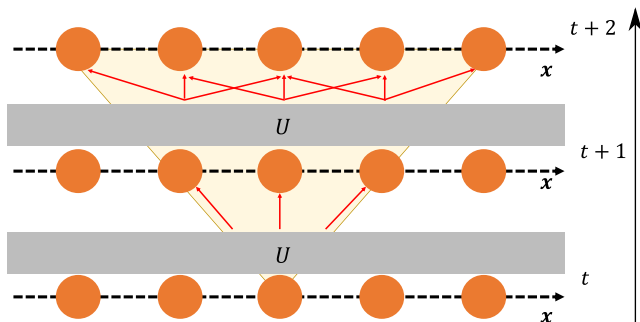


FIG. 1. One-dimensional QCA. Representation of the one-dimensional QCA discrete-time evolution described by the unitary operator U . Here, the quantum field located at each lattice point interacts locally only with the nearest neighbors at each step of the evolution.

regime, regarding microscopy [57,58], optical trapping [59] and communication [60–64], and in quantum information processing for the development of protocols in quantum communication [65–67], computation [68,69], metrology [70–72], and cryptography [73,74]. Moreover, OAM-based platforms offer the possibility to produce a DTQW on a line without an exponential increase of the number of optical elements with respect to the length of the walk [28,31,43–45].

Here, we move beyond the present status of experimental OAM-based quantum walk platforms [28,43–45,53], implementing eight steps of a DTQW with a controllable initial state and an arbitrary projective measurement stage. Our setup allows us to perform a rich dynamics for what concerns both the length of the evolution and the manipulation of the experimental parameters. As a certificate of our simulation, we observed the *Zitterbewegung*, a quivering motion of a relativistic particle that, despite being practically impossible to observe in relativistic systems, is considered as one of their benchmark signatures. Indeed, it was sought in the pioneering—and to date one of the very few—quantum simulations of Dirac equations in a trapped-ion system [75]. We achieved the digital quantum simulation of *Zitterbewegung*. Our work demonstrates the capability of photonic platforms of simulating relativistic behavior, which is difficult to observe in real-case scenarios, paving the way for further experimental implementations of QCA and DQCA, also with more complex evolution dynamics thanks to the reconfigurability of the platform for what concerns input and output stages.

II. QUANTUM CELLULAR AUTOMATA AND QUANTUM WALKS

Quantum cellular automata describe the unitary evolution of a lattice of cells, each representing a quantum system. The evolution occurs in discrete steps and it is *local*, namely, the state of a cell after a certain step $t + 1$ depends only on the state of finitely many neighboring cells after the preceding step t (see Fig. 1).

Let us consider the one-dimensional nearest-neighbor lattice \mathbb{Z} and a local bosonic (fermionic) mode per cell. We associate every site $x \in \mathbb{Z}$ with an algebra of field operators

$\psi_{x,a}$, where the index $a \in S$ belongs to a finite set S and denotes some internal degrees of freedom (e.g., polarization, spin, helicity, ...). The field operators fulfill either the canonical commutation relations (CCR) $[\psi_{x,a}, \psi_{y,b}^\dagger] = \delta_{x,y} \delta_{a,b}$ and $[\psi_{x,a}, \psi_{y,b}] = [\psi_{x,a}^\dagger, \psi_{y,b}^\dagger] = 0$ or the canonical anticommutation relations (CAR) $\{\psi_{x,a}, \psi_{y,b}^\dagger\} = \delta_{x,y} \delta_{a,b}$, $\{\psi_{x,a}, \psi_{y,b}\} = \{\psi_{x,a}^\dagger, \psi_{y,b}^\dagger\} = 0$, $\forall x, y \in \mathbb{Z}$, and $a, b \in S$. A quantum cellular automaton \mathcal{U} is a local and translation invariant automorphism of the representation of the CCR (CAR) algebra which represents a one-step evolution of the lattice. We give a Fock-space representation of the CCR (CAR) algebra by introducing the N -excitation (particle) states $|x_1, a_1\rangle, \dots, |x_N, a_N\rangle := \psi_{x_1, a_1}^\dagger \cdots \psi_{x_N, a_N}^\dagger |\Omega\rangle$, where $|\Omega\rangle$ is the *vacuum state*, i.e., the state with no excitations which obeys $\psi_{x_i, a_i} |\Omega\rangle = 0$ for all i [76]. If we consider the particular case of a free, i.e., non-interacting, evolution, the QCA action is linear in the field operators, namely,

$$\mathcal{U}(\psi_{x,a}) = \sum_{y \in \mathbb{Z}} \sum_{b \in S} U_{y,b;x,a}^* \psi_{y,b}, \quad (1)$$

where the coefficients $U_{y,b;x,a}$ turn out to be matrix elements of a unitary operator on the subspace spanned by single-particle states.

Thus, the dynamics is completely determined by the *quantum walk* U on the single-particle Hilbert space $\mathbb{C}^S \otimes l_2(\mathbb{Z})$:

$$\begin{aligned} |\psi(t+1)\rangle &= U|\psi(t)\rangle, \\ U|a\rangle|x\rangle &= \sum_{y \in \mathbb{Z}} \sum_{b \in S} U_{y,b;x,a} |b\rangle|y\rangle, \\ |a\rangle|x\rangle &= |(x, a)\rangle. \end{aligned} \quad (2)$$

We now consider a two-dimensional internal degree of freedom corresponding to the polarization of an electromagnetic field mode. The Hilbert space \mathbb{C}^2 is thus spanned by the polarization eigenstates, $\{|V\rangle, |H\rangle\}$, and the circularly polarized states are denoted as $|L\rangle$ and $|R\rangle$ with

$$|L\rangle = \frac{1}{\sqrt{2}}(|H\rangle + i|V\rangle), \quad |R\rangle = \frac{1}{\sqrt{2}}(|H\rangle - i|V\rangle).$$

Because the evolution is translationally invariant, it is convenient to represent the unitary operator U in Eq. (2) through the momentum representation:

$$U = \int_{-\pi}^{\pi} dk U(k) \otimes |k\rangle\langle k|, \quad U(k)|\pm\rangle_k = e^{\mp i\omega(k)} |\pm\rangle_k, \quad (3)$$

where we introduced the plane waves $|k\rangle := \sum_x \frac{e^{ikx}}{\sqrt{2\pi}} |x\rangle$, and $U(k) \in \text{SU}(2)$ is a unitary matrix with eigenvectors $|+\rangle_k$ and $|-\rangle_k$ [77]. For example, the DTQW corresponding to the one-particle sector of the Dirac cellular automaton [34,35,55] reads as follows:

$$U(k) = \begin{pmatrix} ne^{-ik} & -im \\ -im & ne^{ik} \end{pmatrix}, \quad \omega(k) = \arccos[n \cos(k)] \quad (4)$$

for some real numbers n and m such that $n^2 + m^2 = 1$.

For a given quantum walk U , it is useful to introduce an *effective Hamiltonian* H which obeys $U = \exp(-iH)$. The Hamiltonian H generates a continuous-time evolution which interpolates the evolution of the quantum walk. We refer to

the support \mathcal{H}_+ (respectively, \mathcal{H}_-) of the projector $P_{\pm} := \int dk |\pm k\rangle\langle\pm k| \otimes |k\rangle\langle k|$ as the subspace of *positive-energy* (respectively, *negative-energy*) states.

In particular, for the DTQW of Eq. (4) we have

$$H = \int_{-\pi}^{\pi} dk H(k) \otimes |k\rangle\langle k|,$$

$$H(k) = \frac{\omega(k)}{\sin \omega(k)} \begin{pmatrix} n \sin(k) & m \\ m & -n \sin(k) \end{pmatrix}, \quad (5)$$

and one can easily verify that for small k and m the one-dimensional Dirac equation

$$i\partial_t \psi(k, t) = (k\sigma_z + m\sigma_x) \psi(k, t) \quad (6)$$

is recovered. The above considerations show that the DTQW in Eq. (4) provides a quantum simulation of the one-dimensional Dirac free field and can be used to observe relativistic quantum effects pertaining to regimes that are difficult to access experimentally.

Zitterbewegung in quantum walks

One of the main predictions of the Dirac equation is the existence of antiparticles. As first noticed by Schrödinger [78], interference of a Dirac particle with its antiparticle is responsible for the so-called *Zitterbewegung* effect, namely, the oscillation of the expected value of the position operator X [33–35, 79–93]. Direct observation of this phenomenon in particle physics would be prohibitive since it requires preparing a coherent superposition of the particle and the antiparticle and the oscillation amplitude is of the order of the Compton wavelength (10^{-12} m for an electron).

Since this phenomenon ultimately depends only on the presence of positive- and negative-energy states, it can be observed also in DTQWs [35]. For the case of a quantum walk on a one-dimensional lattice [see Eq. (3)], the position operator is $X := \sum_{x \in \mathbb{Z}} x I \otimes |x\rangle\langle x|$ and its time evolution $X(t) = U^{-t} X U^t$ can be computed by integrating the differential equation $\frac{d^2}{dt^2} X(t) = -[H, [H, X]]$, where H is the effective Hamiltonian. We obtain

$$X(t) = X(0) + Vt + \frac{1}{2iH} (e^{2iHt} - I)F,$$

$$V := \int_{-\pi}^{\pi} dk \frac{\omega'(k)}{\omega(k)} H(k) \otimes |k\rangle\langle k|, \quad F := [H, X] - V, \quad (7)$$

where V is the velocity operator and F is responsible for the oscillating motion. Since $FP_{\pm} = P_{\mp}F$, we have that the *Zitterbewegung* occurs only for states which are a superposition of positive-energy (particle) and negative-energy (antiparticle) states. Indeed, by taking the expectation value of $X(t)$ with respect to a state $|\psi\rangle = |\psi\rangle_+ + |\psi\rangle_-$, where $|\psi\rangle_{\pm} \in \mathcal{H}_{\pm}$, we have

$$\langle X(t) \rangle = x_+(t) + x_-(t) + x_0 + z(t),$$

$$x_{\pm}(t) := \langle \psi_{\pm} | X(0) + Vt | \psi_{\pm} \rangle,$$

$$x_0 := 2\text{Re}[\langle \psi_+ | X(0) - (2iH)^{-1} F | \psi_- \rangle],$$

$$z(t) := 2\text{Re}[\langle \psi_+ | (2iH)^{-1} e^{2iHt} F | \psi_- \rangle], \quad (8)$$

and we see that interference between positive- and negative-energy states causes a shift x_0 of the mean value of the

position and the oscillating term $z(t)$. Let us now consider states whose particle and antiparticle components are both smoothly peaked around some momentum eigenstate, i.e.,

$$|\psi\rangle_{\text{in}} = c_+ |\psi_+\rangle + c_- |\psi_-\rangle, \quad (9)$$

$$|\psi_{\pm}\rangle = \int \frac{dk}{\sqrt{2\pi}} g(k) |\pm k\rangle |k\rangle, \quad (10)$$

where $|c_+|^2 + |c_-|^2 = 1$ and $|g(k)|^2$ is peaked around k_0 . Therefore, for small value of t , the oscillating terms can be approximated as follows:

$$z(t) = |c_+||c_-| |f(k_0)| \cos[2\omega(k_0)t + \phi_0], \quad (11)$$

where we define $f(k) := \langle +k | F | -k \rangle / [2i\omega(k)]$ and ϕ_0 is a suitable phase.

III. EXPERIMENTAL IMPLEMENTATION OF THE DIRAC CELLULAR AUTOMATON

To experimentally realize the DQCA, we employ the two components of the photon angular momentum, the spin angular momentum and the orbital angular momentum, to encode coin and walker states of a quantum walk, respectively. The orthonormal basis $\{|R\rangle, |L\rangle\}$ corresponds to right- and left-circular polarization, respectively. The position states $\{|x\rangle, x \in \mathbb{Z}\}$ represent eigenstates of the OAM; in particular, throughout the paper we consider its expression in the eigenstate basis of Laguerre-Gaussian modes [94].

In our platform, the polarization can be controlled by a set of waveplates. In the circularly polarized basis $\{|R\rangle, |L\rangle\}$, the action of a quarter-waveplate followed by a half-waveplate can be described by the following unitary matrix:

$$C = \frac{1}{\sqrt{2}} \begin{pmatrix} e^{2i(\alpha-\beta)} & ie^{2i\alpha} \\ ie^{-2i\alpha} & e^{-2i(\alpha-\beta)} \end{pmatrix}, \quad (12)$$

where α and β are the angles of the fast axes with respect to the horizontal axis.

A conditional shift in the OAM (i.e., in the spatial degree of freedom) is implemented using a device called a q-plate [95]. The latter is a thin plate made of a birefringent material with a direction for the optical axis that is not uniform over the device. The angle between the optical axis and the horizontal axis of the device follows the relation $\gamma = \alpha_0 + q\phi$, where α_0 is the initial angle, q is the topological charge of the device, and ϕ is the azimuthal angle on the device plane. The delay introduced on the propagation by such arrangement of the optical axis produces a modulation of the wave front, the q-plate action, in the momentum representation, and can be described by the following unitary operator [95]:

$$Q(k) = \begin{pmatrix} \cos \frac{\delta}{2} & ie^{i2\alpha_0} \sin \frac{\delta}{2} e^{ik} \\ ie^{-i2\alpha_0} \sin \frac{\delta}{2} e^{-ik} & \cos \frac{\delta}{2} \end{pmatrix}, \quad (13)$$

where $k = 2q\phi$ and $\delta \in [0, \pi]$ is the q-plate tuning. The latter is directly linked to the efficiency of the device in the manipulation of the angular momentum of light; this parameter can be electrically tuned to switch on ($\delta = \pi$) or switch off ($\delta = 0$) the device and, thus, control its action.

We realize an eight-step DTQW on a line, where each step is composed of a q-plate and a set of a half-waveplate (HWP)

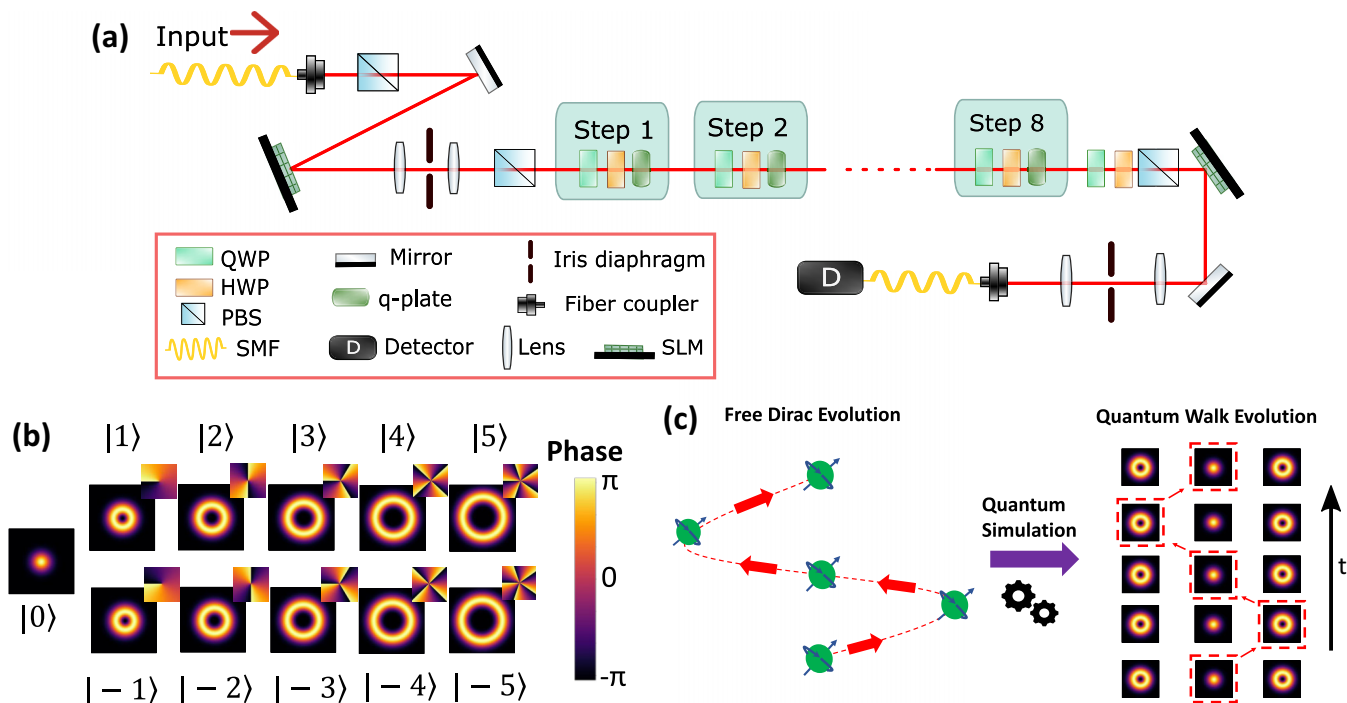


FIG. 2. Experimental setup. (a) The quantum cellular automaton evolution is implemented through an eight-step discrete-time quantum walk in the OAM of light. First of all, single-photon states are generated through spontaneous parametric down-conversion in a PPKTP nonlinear crystal. After projecting the polarization of single photons on the horizontal one through a polarizing beam splitter (PBS), the desired input state is produced via a spatial light modulator (SLM) and, after a spatial filtering performed with an iris diaphragm, is sent to the DTQW. Each step of the latter consists of a coin operator, implemented by a quarter-waveplate (QWP) and a half-waveplate (HWP), and a shift operator performed using a q-plate. Then, the polarization is traced out using a series of QWP, HWP, and PBS. The output-state probability distribution is measured with a projective measurement executed via a further SLM followed by a single-mode fiber (SMF), the resulting coupled signal is detected by an avalanche photodiode detector. (b) Mapping between the OAM space and the position space. In particular, each position of the Dirac particle is identified with a different OAM eigenstate. For the latter, we report both the intensity and the phase of the wave function as expressed in the Laguerre-Gaussian mode basis. (c) The time evolution of a free Dirac particle is simulated through the DTQW platform using the orbital angular momentum of single photons. Here, a modification in the particle position is identified with a variation of the OAM value.

and a quarter-waveplate (QWP). Then, the single step is given by the composition:

$$U(k) = Q(k)C. \quad (14)$$

The entire setup is enclosed between two spatial light modulators (SLMs) as shown in Fig. 2(a), a configuration that has been already proved suitable for the implementation of the DTQW dynamics [43–45]. The inputs of the setup are triggered single-photon states produced via spontaneous parametric down-conversion (SPDC) in a periodically poled potassium titanyl phosphate (PPKTP) nonlinear crystal. These are coupled into a single-mode fiber (SMF) and then sent to the first SLM. The latter is used to modulate the spatial profile of photons to obtain the desired initial state at the entrance of the quantum walk. Therefore, the input states of the setup are of the following factorized form:

$$|\psi\rangle_{\text{in}} = \frac{1}{\sqrt{2}}(|R\rangle + |L\rangle) \otimes \sum_{x \in \mathbb{Z}} g(x)|x\rangle, \quad (15)$$

where $g(x) \in \mathbb{R}$ and $\sum_x |g(x)|^2 = 1$.

A second SLM instead is employed in the measurement stage along with a single-mode fiber to project the output state onto the computational basis and extract the occupation probability of each OAM mode [53,96–100]. Before doing that, the polarization degree of freedom is traced out using a series composed of a QWP, a HWP, and a polarizing beam splitter (PBS). In this way, we are able to measure only the OAM components of the walker state at the end of the DTQW. In particular, the waveplates are used to project the output states on both the two circular polarizations, and the information associated with them is canceled out by summing the photon counts collected in the two cases for each OAM value measured with the SLM.

The discrete size of SLM pixels determines the modulation efficiency of the device especially for high OAM values [96,99], while the divergence of the OAM modes [44,53] needs to be engineered and accounted for depending on the number of steps. In particular, our setup gives us full control over OAM states $|x\rangle$ such that $|x| \leq 5$, and we choose a wave packet which stays confined therein for the whole evolution. Moreover, since the platform performs up to eight evolution steps, it is convenient that the *Zitterbewegung* period

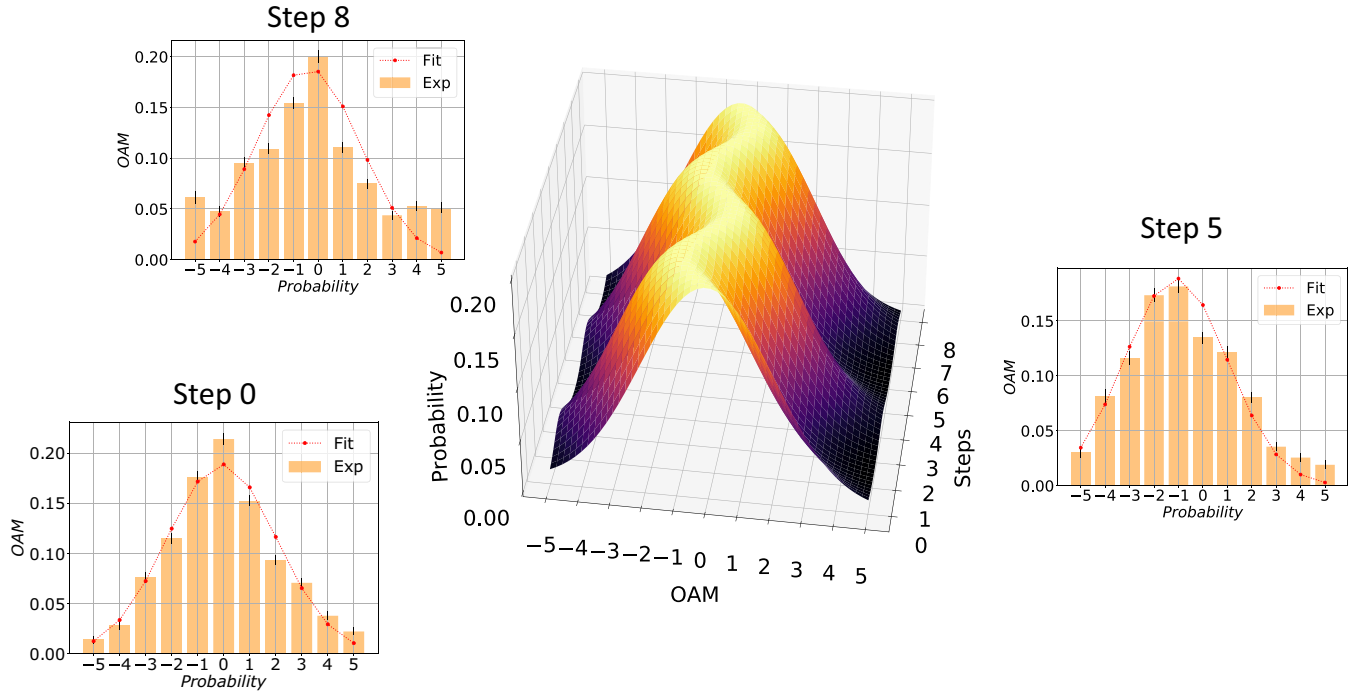


FIG. 3. Data analysis. Representation of the Gaussian fit performed on experimental data. The 3D function shown is obtained by fitting the experimental data with the function in Eq. (18), where the assumed theoretical model is characterized by a Gaussian distribution that oscillates around the initial position during the evolution. In side panels, the comparison between the experimental distribution and the fitted function is reported for three different steps of the evolution (here 0 represents the input state). Although satisfactory similarities can be observed, the difference between histograms and plotted curves increases with the step evolution and this is mainly due to experimental imperfections. The reported errors on experimental data are due to the Poissonian statistics of the measured counts.

$T = 2\pi/2\omega_0$, see Eq. (11), be of the order of 4, so as to observe two complete oscillations.

Let us consider the quantum walk step

$$U(k) = \frac{1}{\sqrt{2}} \begin{pmatrix} e^{ik} & e^{ik} \\ -e^{-ik} & e^{-ik} \end{pmatrix}, \quad (16)$$

which can be experimentally implemented by choosing the following parameters: $\delta = \pi$, $\alpha_0 = \pi/4$, $\alpha = -\pi/4$, and $\beta = \pi/4$ in Eq. (14). One can show that the dispersion relation $\omega(k)$ of $U(k)$ is equivalent to that characterizing Eq. (4) for $m = n = \sqrt{2}/2$. We are then interested in those states that are superpositions of positive- and negative-energy eigenstates and that at the peak angular wave number k_0 feature the following: (i) zero group velocity $\omega'(k_0) = \partial_k \omega(k_0) = 0$, (ii) angular frequency equal to $\pi/4$, and (iii) appreciable *Zitterbewegung* amplitude given by $|c_+| = |c_-| = 1/\sqrt{2}$ and $|f(k_0)| = 1$ [see Eq. (11)]. We selected the initial state

$$|\psi\rangle_{\text{in}} = \frac{1}{\sqrt{2}}(|R\rangle + |L\rangle) \otimes \sum_{x \in \mathbb{Z}} G_{x_0, \sigma}(x)|x\rangle, \quad (17)$$

where $G_{x_0, \sigma}(x)$ is the truncated normal distribution between -5 and 5 , centered in $x_0 = 0$, and with the standard deviation $\sigma = 3.0$. For such a spatial distribution, the wave function in momentum representation resembles a normal distribution peaked at $k_0 = 0$ and with the standard deviation $1/\sigma = 1/3$.

This setup allows us to have precise control and reproduce the Dirac evolution step-by-step by simply turning on the right number of q-plates.

IV. RESULTS

Exploiting the DTQW dynamics implemented with the setup, we are able to realize a photonic QCA that allows us to experimentally study the *Zitterbewegung* effect of the Dirac relativistic evolution in the space of the single-photon OAM. To this aim, we use q-plates with the topological charge $q = 1/2$ and select the angles of the waveplates in order to reproduce the evolution operator reported in Eq. (16). Notably, we realized a state-of-the-art platform able to reach eight steps of the DQCA evolution for arbitrary initial states in dimension 11.

We simulated the oscillatory behavior of the position of a one-dimensional relativistic particle encoding this degree of freedom in the OAM of photons, thus making the relation $|x\rangle = |m\rangle$, where x is the position and m is the value of the OAM. This encoding is explicitly reported in Fig. 2(b), while a conceptual representation of the simulation approach implemented in this work is shown in Fig. 2(c). We considered as input a Gaussian state localized around the position $|0\rangle$, generated using the first SLM in Fig. 2(a), and observed its evolution step by step. In particular, for each step we turned on the relative q-plate setting $\delta = \pi$, traced out the information stored in the polarization, and measured via the second SLM and the SMF the walker-state distribution over the computational basis $\{|i\rangle\}_{i=-5}^5$, opportunely taking into account the efficiencies of the measurement holograms [96,99]. From the measurements, we extracted the occupation probabilities of each site and derived the evolution of the mean position (see

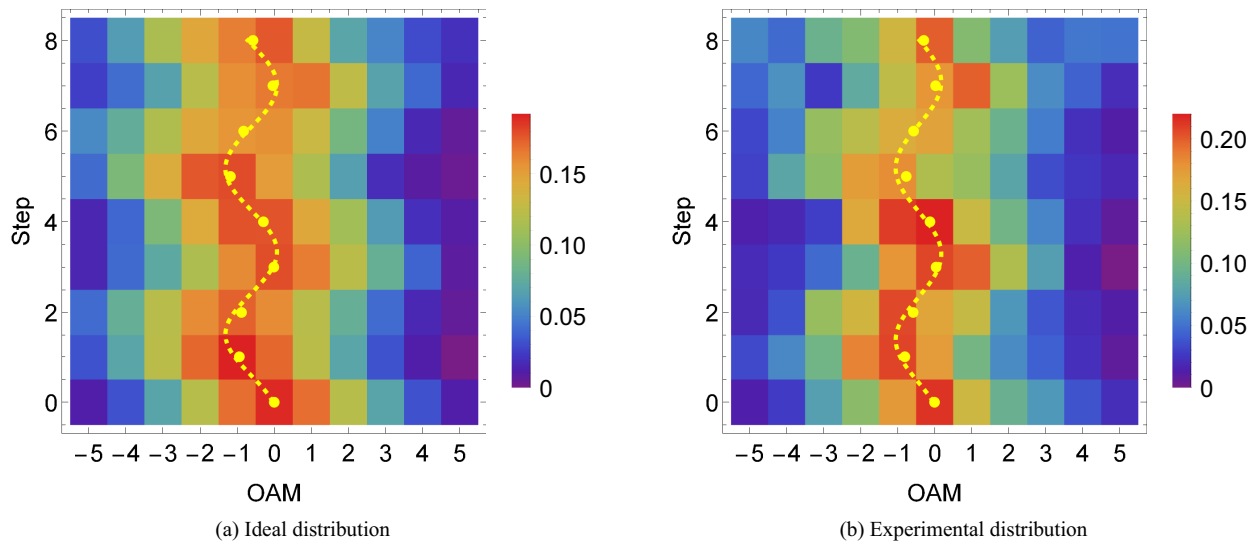


FIG. 4. *Zitterbewegung* dynamics. The plots show the output-state distribution over the OAM computational basis for each time step considered; we indicate with 0 the initial input state. Panel (a) shows the evolution obtained following the ideal noiseless model of the quantum walk, and in panel (b) experimental data are shown. Yellow points represent the behavior of the mean position during the steps of the evolution, while the dashed line is obtained as the step-dependent mean values of the fitted Gaussian functions.

the Appendix for the measured distribution at each step and the corresponding theoretical model). In particular, from a theoretical prospective, we expect a Gaussian distribution that oscillates around the position $x = 0$ during the evolution. The oscillation of the Gaussian peak follows the sinusoidal expression in Eq. (11) with the frequency $\omega = 2\omega(k_0) = \pi/2$ and the amplitude $A = |c_+||c_-||f(k_0)| = 0.5$. Since, in the experiment, we only had access to the portion of the distribution between $x = -5$ and $x = 5$, the reference values for ω and A were different. Therefore, at each step, we performed a fit over the distributions in a truncated interval of the position space spanned by $x \in [-5, 5]$ with Gaussian functions whose mean values oscillated along the evolution direction:

$$f(t, y) = \frac{e^{-(y-\mu_0-A \cos(\omega t+\phi))^2/(2\sigma^2)}}{\sigma\sqrt{2\pi}}, \quad (18)$$

where t represents the step of the DTQW, y the values of probability distributions over the OAM basis, μ_0 the mean of the Gaussian distribution, and σ its standard deviation. This fitting procedure was used to derive the oscillation parameters for both theoretical and experimental distributions. The results in the experimental case are shown in Fig. 3, where the 3D plot reports the time evolution of the fitted Gaussian envelopes.

The complete experimental results are reported in Fig. 4 together with the theoretical ideal distributions. The yellow dashed lines represent the oscillations of the mean values of the fitted Gaussian functions. For the theoretical distribution, the sinusoidal curve in Fig. 4(a) is characterized by values equal to $\omega = 1.714 \pm 0.017$ and $A = 0.695 \pm 0.032$. Experimentally, we obtained an oscillation very similar to the expected one with values that correspond to $\omega = 1.655 \pm 0.009$ and $A = 0.615 \pm 0.017$, the measured behavior is reported in [Fig. 4(b)]. From both numerical results and plots shown in Fig. 4, it can be seen how the implemented platform is capable of simulating the dynamics of a free

relativistic particle, reproducing its typical *Zitterbewegung* trembling motion.

V. CONCLUSIONS

We showcase the photonic implementation of a quantum cellular automaton able to simulate features typical of the Dirac free-particle evolution. Our work makes a relevant step forward in the exploration of experimental QCA, and especially of DQCA, in photonic platforms. The single-particle sector of the DQCA is realized through the discrete-time quantum walk dynamics performed exploiting the OAM of single photons. In particular, the quantum walk platform is composed of a cascade of eight q-plates interspaced by waveplates and placed between 2 SLMs. This setup allowed us to have a high degree of control over the input state and the capability to perform the eight steps of the automaton evolution. The simulation power of the DQCA was used to reproduce the *Zitterbewegung*, i.e., the trembling motion that occurs during the free evolution of relativistic particles. These effects are clearly reproduced in the reported results, in which the particle position, encoded in the OAM value of single photons, presents an oscillatory behavior with an amplitude and a frequency in agreement with the theoretical predictions. Moreover, these experimental results represent a proof of principle demonstrating the possibility of employing photonic platforms to implement DQCAs. The proposed experimental protocol constitutes a first step towards the simulation of more complex dynamics where position-dependent evolutions are necessary, such as the Dirac particle evolution subject to external potential [16,101] and curved space-time [15,102,103]. On the other side, the potential of the implemented DQCA can be extended to the multiparticle regimes, for instance, by considering entangled photons in parallel quantum walks [104]. Although the DTQW dynamics is a special case of

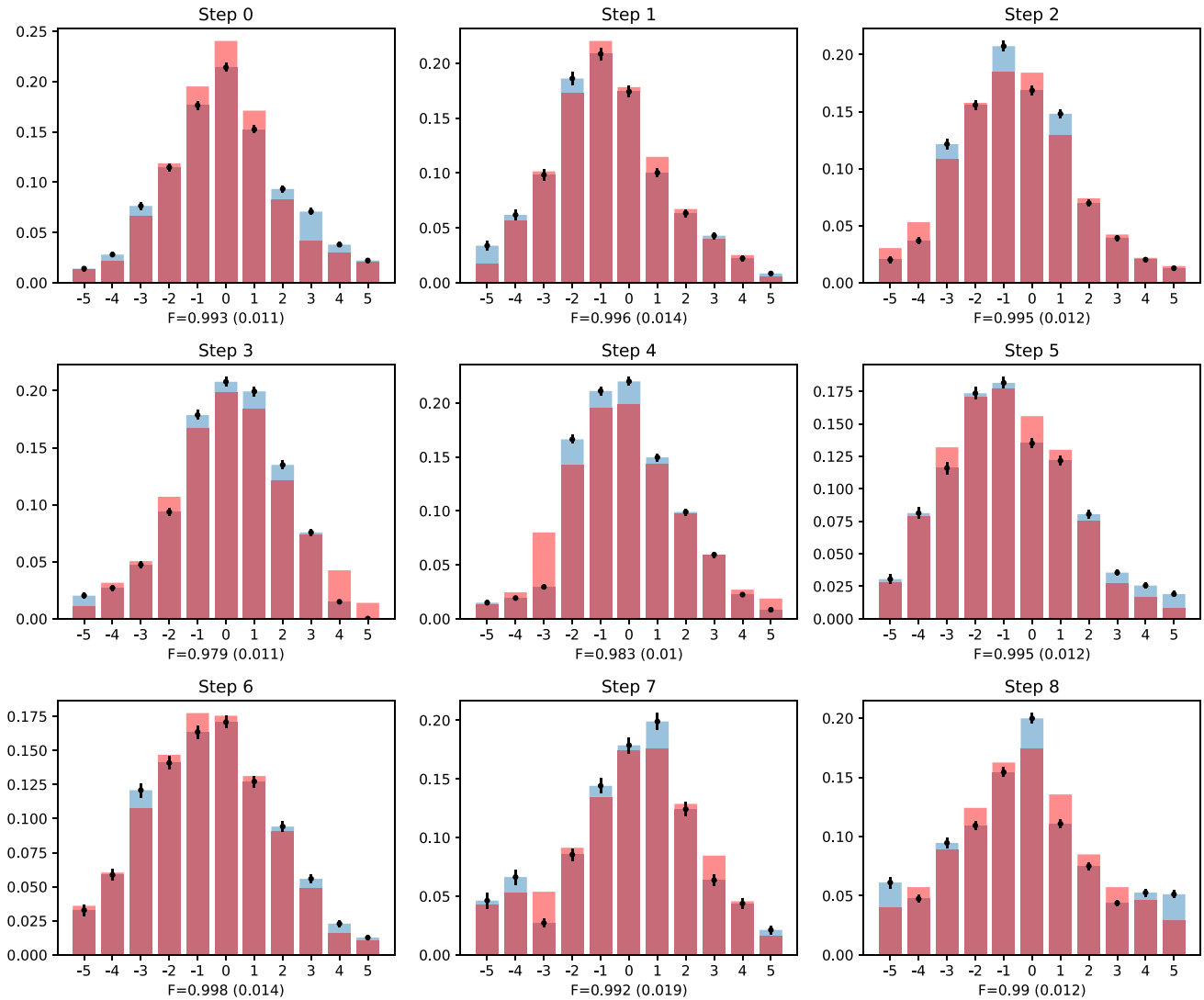


FIG. 5. Step-by-step QCA evolution. OAM occupation probability measured at the output of the setup for different steps of the DTQW dynamics. Above each histogram the relative step is indicated. The experimental data are reported in blue, while in red are reported the expected behaviors from the theoretical noisy model of the experimental apparatus. The fidelity between the experimental and theoretical distributions is reported under each histogram. Error bars are due to the Poissonian statistics of single-photon counting.

QCA evolution, the provided photonics tools are completely general and thus can aim at the implementation of more general multidimensional QCA in suitable experimental photonics platforms.

ACKNOWLEDGMENTS

P.P. and F.S. acknowledge financial support from European Union–Next Generation EU through the MUR project Progetti di Ricerca d’Interesse Nazionale (PRIN) QCAPP Project No. 2022LCEA9Y. F.S. also acknowledge support from the Templeton Foundation, The Quantum Information Structure of Spacetime (QISS2) Project (qiss.fr) Grant Agreement No. 62312. A.B. acknowledges financial support from European Union–Next Generation EU through the PNNR MUR Project No. PE0000023-NQSTI. The opinions expressed in this pub-

lication are those of the authors and do not necessarily reflect the views of the John Templeton Foundation.

APPENDIX: NOISY THEORETICAL MODEL AND EXPERIMENTAL DATA

In this section, we present in more detail the experimental result of the QCA evolution together with the theoretical model used to account for the experimental imperfections present in the setup. These are mainly related to the nonunitary efficiencies of the cascaded q-plates, errors in the coin operators and the efficiencies of the holographic technique in manipulating the OAM [96,99]. In this way, the DTQW evolution is simulated by means of a theoretical model whose parameters are the conversion efficiencies of the q-plates, the offset of the waveplates and the efficiencies of

the two SLMs. These parameters are optimized around the attended values by simultaneously minimizing the square difference between the theoretical evolution and the raw measured data for each step. All the experimental distributions, measured at each step, are shown in Fig. 5, where the OAM

probability occupation, as expected from the noisy theoretical model and the experimental unfolded one, is reported. The similarity between the theoretical and experimental distributions is quantified by the fidelity value reported under each histogram.

-
- [1] J. von Neumann, *Theory of Self-Reproducing Automata*, edited by A. W. Burks (University of Illinois, Champaign, IL, 1966).
- [2] B. Schumacher and R. F. Werner, Reversible quantum cellular automata, [arXiv:quant-ph/0405174](https://arxiv.org/abs/quant-ph/0405174).
- [3] D. Gross, V. Nesme, H. Vogts, and R. F. Werner, Index theory of one dimensional quantum walks and cellular automata, *Commun. Math. Phys.* **310**, 419 (2012).
- [4] P. Arrighi, V. Nesme, and R. Werner, Unitarity plus causality implies localizability, *J. Comput. Syst. Sci.* **77**, 372 (2011).
- [5] T. Farrelly, A review of quantum cellular automata, *Quantum* **4**, 368 (2020).
- [6] M. Freedman and M. B. Hastings, Classification of quantum cellular automata, *Commun. Math. Phys.* **376**, 1171 (2020).
- [7] R. P. Feynman, Simulating physics with computers, in *Feynman and Computation*, edited by Tony Hey (CRC, Boca Raton, FL, 1982), pp. 133–153.
- [8] J. Watrous, On one-dimensional quantum cellular automata, in *Proceedings of IEEE 36th Annual Foundations of Computer Science* (IEEE, New York, 1995), pp. 528–537.
- [9] R. Raussendorf, Quantum cellular automaton for universal quantum computation, *Phys. Rev. A* **72**, 022301 (2005).
- [10] K. G. H. Vollbrecht and J. I. Cirac, Reversible universal quantum computation within translation-invariant systems, *Phys. Rev. A* **73**, 012324 (2006).
- [11] P. Arrighi and J. Grattage, The quantum game of life, *Phys. World* **25**, 23 (2012).
- [12] H. C. Po, L. Fidkowski, T. Morimoto, A. C. Potter, and A. Vishwanath, Chiral floquet phases of many-body localized bosons, *Phys. Rev. X* **6**, 041070 (2016).
- [13] L. Fidkowski, H. C. Po, A. C. Potter, and A. Vishwanath, Interacting invariants for floquet phases of fermions in two dimensions, *Phys. Rev. B* **99**, 085115 (2019).
- [14] T. J. Osborne, Efficient approximation of the dynamics of one-dimensional quantum spin systems, *Phys. Rev. Lett.* **97**, 157202 (2006).
- [15] G. Di Molfetta, M. Brachet, and F. Debbasch, Quantum walks as massless Dirac fermions in curved space-time, *Phys. Rev. A* **88**, 042301 (2013).
- [16] C. Cedzich, T. Rybár, A. H. Werner, A. Alberti, M. Genske, and R. F. Werner, Propagation of quantum walks in electric fields, *Phys. Rev. Lett.* **111**, 160601 (2013).
- [17] G. Di Molfetta, M. Brachet, and F. Debbasch, Quantum walks in artificial electric and gravitational fields, *Physica A: Statistical Mechanics and its Applications* **397**, 157 (2014).
- [18] G. M. D’Ariano, N. Mosco, P. Perinotti, and A. Tosini, Discrete Feynman propagator for the Weyl quantum walk in $2 + 1$ dimensions, *Europhys. Lett.* **109**, 40012 (2015).
- [19] A. Bisio, N. Mosco, and P. Perinotti, Scattering and perturbation theory for discrete-time dynamics, *Phys. Rev. Lett.* **126**, 250503 (2021).
- [20] L. Piroli and J. I. Cirac, Quantum cellular automata, tensor networks, and area laws, *Phys. Rev. Lett.* **125**, 190402 (2020).
- [21] D. Deutsch, Quantum theory, the Church–Turing principle and the universal quantum computer, *Proc. R. Soc. London, Ser. A* **400**, 97 (1985).
- [22] A. Ambainis, E. Bach, A. Nayak, A. Vishwanath, and J. Watrous, One-dimensional quantum walks, in *STOC ’01 Proceedings of the Thirty-Third Annual ACM Symposium on Theory of Computing* (ACM, New York, 2001), pp. 37–49.
- [23] N. Shenvi, J. Kempe, and K. Birgitta Whaley, Quantum random-walk search algorithm, *Phys. Rev. A* **67**, 052307 (2003).
- [24] J. Kempe, Quantum random walks: An introductory overview, *Contemp. Phys.* **44**, 307 (2003).
- [25] A. Ambainis, J. Kempe, and A. Rivosh, Coins make quantum walks faster, in *Proceedings of the Sixteenth Annual ACM-SIAM Symposium on Discrete Algorithms* (Society for Industrial and Applied Mathematics, Philadelphia, 2005), pp. 1099–1108.
- [26] R. Portugal, *Quantum Walks and Search Algorithms*, Quantum Science and Technology (Springer New York, 2013).
- [27] W.-W. Zhang, S. K. Goyal, C. Simon, and B. C. Sanders, Decomposition of split-step quantum walks for simulating Majorana modes and edge states, *Phys. Rev. A* **95**, 052351 (2017).
- [28] F. Cardano, M. Maffei, F. Massa, B. Piccirillo, C. de Lisio, G. D. Filippis, V. Cataudella, E. Santamato, and L. Marrucci, Statistical moments of quantum-walk dynamics reveal topological quantum transitions, *Nat. Commun.* **7**, 11439 (2016).
- [29] T. Kitagawa, M. S. Rudner, E. Berg, and E. Demler, Exploring topological phases with quantum walks, *Phys. Rev. A* **82**, 033429 (2010).
- [30] L. Xiao, X. Zhan, Z. H. Bian, K. K. Wang, X. Zhang, X. P. Wang, J. Li, K. Mochizuki, D. Kim, N. Kawakami, W. Yi, H. Obuse, B. C. Sanders, and P. Xue, Observation of topological edge states in parity-time-symmetric quantum walks, *Nat. Phys.* **13**, 1117 (2017).
- [31] F. Cardano, A. D’Errico, A. Dauphin, M. Maffei, B. Piccirillo, C. de Lisio, G. De Filippis, V. Cataudella, E. Santamato, L. Marrucci, M. Lewenstein, and P. Massignan, Detection of Zak phases and topological invariants in a chiral quantum walk of twisted photons, *Nat. Commun.* **8**, 15516 (2017).
- [32] X. Zhan, L. Xiao, Z. Bian, K. Wang, X. Qiu, B. C. Sanders, W. Yi, and P. Xue, Detecting topological invariants in nonunitary discrete-time quantum walks, *Phys. Rev. Lett.* **119**, 130501 (2017).
- [33] P. Kurzyński, Relativistic effects in quantum walks: Klein’s paradox and zitterbewegung, *Phys. Lett. A* **372**, 6125 (2008).
- [34] A. Mallick and C. Chandrashekar, Dirac cellular automaton from split-step quantum walk, *Sci. Rep.* **6**, 25779 (2016).

- [35] A. Bisio, G. M. D'Ariano, and A. Tosini, Dirac quantum cellular automaton in one dimension: *Zitterbewegung* and scattering from potential, *Phys. Rev. A* **88**, 032301 (2013).
- [36] G. M. D'Ariano and P. Perinotti, Derivation of the Dirac equation from principles of information processing, *Phys. Rev. A* **90**, 062106 (2014).
- [37] A. Bisio, G. M. D'Ariano, and P. Perinotti, Quantum cellular automaton theory of light, *Ann. Phys.* **368**, 177 (2016).
- [38] A. Bisio, G. M. D'Ariano, and P. Perinotti, Special relativity in a discrete quantum universe, *Phys. Rev. A* **94**, 042120 (2016).
- [39] M. Karski, L. Förster, J. Choi, A. Steffen, W. Alt, D. Meschede, and A. Widera, Quantum walk in position space with single optically trapped atoms, *Science* **325**, 174 (2009).
- [40] H. Schmitz, R. Matjeschk, C. Schneider, J. Glueckert, M. Enderlein, T. Huber, and T. Schaetz, Quantum walk of a trapped ion in phase space, *Phys. Rev. Lett.* **103**, 090504 (2009).
- [41] F. Zähringer, G. Kirchmair, R. Gerritsma, E. Solano, R. Blatt, and C. F. Roos, Realization of a quantum walk with one and two trapped ions, *Phys. Rev. Lett.* **104**, 100503 (2010).
- [42] L. Sansoni, F. Sciarrino, G. Vallone, P. Mataloni, A. Crespi, R. Ramponi, and R. Osellame, Two-particle bosonic-fermionic quantum walk via integrated photonics, *Phys. Rev. Lett.* **108**, 010502 (2012).
- [43] T. Giordani, E. Polino, S. Emiliani, A. Suprano, L. Innocenti, H. Majury, L. Marrucci, M. Paternostro, A. Ferraro, N. Spagnolo, and F. Sciarrino, Experimental engineering of arbitrary qudit states with discrete-time quantum walks, *Phys. Rev. Lett.* **122**, 020503 (2019).
- [44] F. Cardano, F. Massa, H. Qassim, E. Karimi, S. Slussarenko, D. Paparo, C. de Lisio, F. Sciarrino, E. Santamato, R. W. Boyd, and L. Marrucci, Quantum walks and wavepacket dynamics on a lattice with twisted photons, *Sci. Adv.* **1**, e1500087 (2015).
- [45] A. Suprano, D. Zia, E. Polino, T. Giordani, L. Innocenti, A. Ferraro, M. Paternostro, N. Spagnolo, and F. Sciarrino, Dynamical learning of a photonics quantum-state engineering process, *Adv. Photonics* **3**, 066002 (2021).
- [46] A. Crespi, R. Osellame, R. Ramponi, V. Giovannetti, R. Fazio, L. Sansoni, F. D. Nicola, F. Sciarrino, and P. Mataloni, Anderson localization of entangled photons in an integrated quantum walk, *Nat. Photon.* **7**, 322 (2013).
- [47] F. Caruso, A. Crespi, A. G. Ciriolo, F. Sciarrino, and R. Osellame, Fast escape of a quantum walker from an integrated photonic maze, *Nat. Commun.* **7**, 11682 (2016).
- [48] T. Kitagawa, M. A. Broome, A. Fedrizzi, M. S. Rudner, E. Berg, I. Kassal, A. Aspuru-Guzik, E. Demler, and A. G. White, Observation of topologically protected bound states in photonic quantum walks, *Nat. Commun.* **3**, 882 (2012).
- [49] J. O. Owens, M. A. Broome, D. N. Biggerstaff, M. E. Goggin, A. Fedrizzi, T. Linjordet, M. Ams, G. D. Marshall, J. Twamley, M. J. Withford, and A. G. White, Two-photon quantum walks in an elliptical direct-write waveguide array, *New J. Phys.* **13**, 075003 (2011).
- [50] X. Qiang, T. Loke, A. Montanaro, K. Aungkunsiri, X. Zhou, J. L. O'Brien, J. Wang, and J. C. F. Matthews, Efficient quantum walk on a quantum processor, *Nat. Commun.* **7**, 11511 (2016).
- [51] J. Boutari, A. Feizpour, S. Barz, C. D. Franco, M. S. Kim, W. S. Kolthammer, and I. A. Walmsley, Large scale quantum walks by means of optical fiber cavities, *J. Opt.* **18**, 094007 (2016).
- [52] C. Esposito, M. R. Barros, A. Durán Hernández, G. Carvacho, F. Di Colandrea, R. Barboza, F. Cardano, N. Spagnolo, L. Marrucci, and F. Sciarrino, Quantum walks of two correlated photons in a 2D synthetic lattice, *npj Quantum Inf.* **8**, 34 (2022).
- [53] A. Suprano, D. Zia, E. Polino, T. Giordani, L. Innocenti, M. Paternostro, A. Ferraro, N. Spagnolo, and F. Sciarrino, Enhanced detection techniques of orbital angular momentum states in the classical and quantum regimes, *New J. Phys.* **23**, 073014 (2021).
- [54] G. M. D'Ariano, The quantum field as a quantum computer, *Phys. Lett. A* **376**, 697 (2012).
- [55] A. Bisio, G. M. D'Ariano, and A. Tosini, Quantum field as a quantum cellular automaton: The Dirac free evolution in one dimension, *Ann. Phys.* **354**, 244 (2015).
- [56] C. H. Alderete, S. Singh, N. H. Nguyen, D. Zhu, R. Balu, C. Monroe, C. Chandrashekar, and N. M. Linke, Quantum walks and Dirac cellular automata on a programmable trapped-ion quantum computer, *Nat. Commun.* **11**, 3720 (2020).
- [57] S. Fühapter, A. Jesacher, S. Bernet, and M. Ritsch-Marte, Spiral phase contrast imaging in microscopy, *Opt. Express* **13**, 689 (2005).
- [58] F. Tamburini, G. Anzolin, G. Umbricco, A. Bianchini, and C. Barbieri, Overcoming the Rayleigh criterion limit with optical vortices, *Phys. Rev. Lett.* **97**, 163903 (2006).
- [59] Q. Zhan, Trapping metallic Rayleigh particles with radial polarization, *Opt. Express* **12**, 3377 (2004).
- [60] A. E. Willner, H. Huang, Y. Yan, Y. Ren, N. Ahmed, G. Xie, C. Bao, L. Li, Y. Cao, Z. Zhao *et al.*, Optical communications using orbital angular momentum beams, *Adv. Opt. Photonics* **7**, 66 (2015).
- [61] N. Bozinovic, Y. Yue, Y. Ren, M. Tur, P. Kristensen, H. Huang, A. E. Willner, and S. Ramachandran, Terabit-scale orbital angular momentum mode division multiplexing in fibers, *Science* **340**, 1545 (2013).
- [62] M. Malik, M. O'Sullivan, B. Rodenburg, M. Mirhosseini, J. Leach, M. P. Lavery, M. J. Padgett, and R. W. Boyd, Influence of atmospheric turbulence on optical communications using orbital angular momentum for encoding, *Opt. Express* **20**, 13195 (2012).
- [63] J. Baghdady, K. Miller, K. Morgan, M. Byrd, S. Osler, R. Ragusa, W. Li, B. M. Cochenour, and E. G. Johnson, Multi-gigabit/s underwater optical communication link using orbital angular momentum multiplexing, *Opt. Express* **24**, 9794 (2016).
- [64] J. Wang, Advances in communications using optical vortices, *Photonics Res.* **4**, B14 (2016).
- [65] X.-L. Wang, X.-D. Cai, Z.-E. Su, M.-C. Chen, D. Wu, L. Li, N.-L. Liu, C.-Y. Lu, and J.-W. Pan, Quantum teleportation of multiple degrees of freedom of a single photon, *Nature (London)* **518**, 516 (2015).
- [66] D. Cozzolino, B. Da Lio, D. Bacco, and L. K. Oxenløwe, High-dimensional quantum communication: Benefits, progress, and future challenges, *Adv. Quantum Technol.* **2**, 1900038 (2019).
- [67] D. Cozzolino, E. Polino, M. Valeri, G. Carvacho, D. Bacco, N. Spagnolo, L. K. Oxenløwe, and F. Sciarrino, Air-core fiber

- distribution of hybrid vector vortex-polarization entangled states, *Adv. Photonics* **1**, 046005 (2019).
- [68] B. P. Lanyon, M. Barbieri, M. P. Almeida, T. Jennewein, T. C. Ralph, K. J. Resch, G. J. Pryde, J. L. O'Brien, A. Gilchrist, and A. G. White, Simplifying quantum logic using higher-dimensional Hilbert spaces, *Nat. Phys.* **5**, 134 (2009).
- [69] T. C. Ralph, K. J. Resch, and A. Gilchrist, Efficient Toffoli gates using qudits, *Phys. Rev. A* **75**, 022313 (2007).
- [70] V. D'Ambrosio, N. Spagnolo, L. Del Re, S. Slussarenko, Y. Li, L. C. Kwek, L. Marrucci, S. P. Walborn, L. Aolita, and F. Sciarrino, Photonic polarization gears for ultra-sensitive angular measurements, *Nat. Commun.* **4**, 2432 (2013).
- [71] R. Fickler, R. Lapkiewicz, W. N. Plick, M. Krenn, C. Schaeff, S. Ramelow, and A. Zeilinger, Quantum entanglement of high angular momenta, *Science* **338**, 640 (2012).
- [72] V. Cimini, E. Polino, F. Belliardo, F. Hoch, B. Piccirillo, N. Spagnolo, V. Giovannetti, and F. Sciarrino, Experimental metrology beyond the standard quantum limit for a wide resources range, *npj Quantum Inf.* **9**, 20 (2023).
- [73] M. Mirhosseini, O. S. Magaña-Loaiza, M. N. O'Sullivan, B. Rodenburg, M. Malik, M. P. J. Lavery, M. J. Padgett, D. J. Gauthier, and R. W. Boyd, High-dimensional quantum cryptography with twisted light, *New J. Phys.* **17**, 033033 (2015).
- [74] F. Bouchard, A. Sit, F. Hufnagel, A. Abbas, Y. Zhang, K. Heshami, R. Fickler, C. Marquardt, G. Leuchs, R. W. Boyd, and E. Karimi, Quantum cryptography with twisted photons through an outdoor underwater channel, *Opt. Express* **26**, 22563 (2018).
- [75] R. Gerritsma, G. Kirchmair, F. Zähringer, E. Solano, R. Blatt, and C. Roos, Quantum simulation of the Dirac equation, *Nature (London)* **463**, 68 (2010).
- [76] We defined the vacuum state as the one with no *localized* excitations. In quantum field theory one usually defines the vacuum state as the ground state of a free Hamiltonian which is a collection of harmonic oscillators. There, particles do not have localized excitation but they have a well-defined energy and momentum (as improper eigestates). Since we will consider the free evolution of a single particle, the difference between the two constructions is immaterial. We chose the local excitation basis for convenience.
- [77] In general, $U(k)$ can have determinant which depends on k . However, one can prove that every DTQW can be decomposed in terms of left (right) shifts on the lattice and DTQWs such that $U(k) \in \text{SU}(2)$ for all k [3].
- [78] E. Schrödinger, *Über die Kräftefreie Bewegung in der Relativistischen Quantenmechanik* (Akademie der wissenschaften in kommission bei W. de Gruyter u. Company, Berlin, 1930).
- [79] B. Thaller, *The Dirac Equation* (Springer, Berlin, 2013).
- [80] G. Dávid and J. Cserti, General theory of Zitterbewegung, *Phys. Rev. B* **81**, 121417(R) (2010).
- [81] J. A. Lock, The Zitterbewegung of a free localized Dirac particle, *Am. J. Phys.* **47**, 797 (1979).
- [82] S. Ahrens, S.-Y. Zhu, J. Jiang, and Y. Sun, Simulation of Zitterbewegung by modelling the Dirac equation in metamaterials, *New J. Phys.* **17**, 113021 (2015).
- [83] S. N. Juneghani, M. Bagheri, and B. Shokri, Study Zitterbewegung effect in a quasi one-dimensional relativistic quantum plasma by Dirac-Heisenberg-Wigner formalization, *J. Cosmol. Astropart. Phys.* **09** (2021) 002.
- [84] L. Lamata, J. León, T. Schätz, and E. Solano, Dirac equation and quantum relativistic effects in a single trapped ion, *Phys. Rev. Lett.* **98**, 253005 (2007).
- [85] T. X. Tran, S. Longhi, and F. Biancalana, Optical analogue of relativistic Dirac solitons in binary waveguide arrays, *Ann. Phys.* **340**, 179 (2014).
- [86] J. Pedernales, R. Di Candia, D. Ballester, and E. Solano, Quantum simulations of relativistic quantum physics in circuit QED, *New J. Phys.* **15**, 055008 (2013).
- [87] W. Zawadzki and T. M. Rusin, Zitterbewegung (trembling motion) of electrons in semiconductors: A review, *J. Phys.: Condens. Matter* **23**, 143201 (2011).
- [88] J. Schliemann, D. Loss, and R. M. Westervelt, Zitterbewegung of electronic wave packets in III-V zinc-blende semiconductor quantum wells, *Phys. Rev. Lett.* **94**, 206801 (2005).
- [89] J. Y. Vaishnav and C. W. Clark, Observing Zitterbewegung with ultracold atoms, *Phys. Rev. Lett.* **100**, 153002 (2008).
- [90] X. Zhang, Observing Zitterbewegung for photons near the dirac point of a two-dimensional photonic crystal, *Phys. Rev. Lett.* **100**, 113903 (2008).
- [91] Q. Liang, Y. Yan, and J. Dong, Zitterbewegung in the honeycomb photonic lattice, *Opt. Lett.* **36**, 2513 (2011).
- [92] H. Deng, F. Ye, B. A. Malomed, X. Chen, and N. C. Panoiu, Optically and electrically tunable Dirac points and Zitterbewegung in graphene-based photonic superlattices, *Phys. Rev. B* **91**, 201402(R) (2015).
- [93] D.-w. Zhang, Z.-d. Wang, and S.-l. Zhu, Relativistic quantum effects of Dirac particles simulated by ultracold atoms, *Front. Phys.* **7**, 31 (2012).
- [94] L. Allen, M. W. Beijersbergen, R. J. C. Spreeuw, and J. P. Woerdman, Orbital angular momentum of light and the transformation of Laguerre-Gaussian laser modes, *Phys. Rev. A* **45**, 8185 (1992).
- [95] L. Marrucci, C. Manzo, and D. Paparo, Optical spin-to-orbital angular momentum conversion in inhomogeneous anisotropic media, *Phys. Rev. Lett.* **96**, 163905 (2006).
- [96] E. Bolduc, N. Bent, E. Santamato, E. Karimi, and R. W. Boyd, Exact solution to simultaneous intensity and phase encryption with a single phase-only hologram, *Opt. Lett.* **38**, 3546 (2013).
- [97] A. Mair, A. Vaziri, G. Weihs, and A. Zeilinger, Entanglement of the orbital angular momentum states of photons, *Nature (London)* **412**, 313 (2001).
- [98] A. Forbes, A. Dudley, and M. McLaren, Creation and detection of optical modes with spatial light modulators, *Adv. Opt. Photonics* **8**, 200 (2016).
- [99] H. Qassim, F. M. Miatto, J. P. Torres, M. J. Padgett, E. Karimi, and R. W. Boyd, Limitations to the determination of a Laguerre-Gauss spectrum via projective, phase-flattening measurement, *J. Opt. Soc. Am. B* **31**, A20 (2014).
- [100] F. Bouchard, N. H. Valencia, F. Brandt, R. Fickler, M. Huber, and M. Malik, Measuring azimuthal and radial modes of photons, *Opt. Express* **26**, 31925 (2018).
- [101] C. Cedzich, T. Geib, A. Werner, and R. Werner, Quantum walks in external gauge fields, *J. Math. Phys.* **60**, 012107 (2019).

- [102] P. Arrighi, S. Facchini, and M. Forets, Quantum walking in curved spacetime, [Quantum Inf. Proc.](#) **15**, 3467 (2016).
- [103] A. Mallick, S. Mandal, A. Karan, and C. M. Chandrashekar, Simulating Dirac Hamiltonian in curved space-time by split-step quantum walk, [J. Phys. Commun.](#) **3**, 015012 (2019).
- [104] T. Giordani, L. Innocenti, A. Suprano, E. Polino, M. Paternostro, N. Spagnolo, F. Sciarrino, and A. Ferraro, Entanglement transfer, accumulation and retrieval via quantum-walk-based qubit–qudit dynamics, [New J. Phys.](#) **23**, 023012 (2021).